Int. J. Electrochem. Sci., 12 **(2017)** 8564 – 8577, doi: 10.20964/2017.09.44

International Journal of
ELECTROCHEMICAL
SCIENCE
www.electrochemsci.org

Direct and Indirect Electrochemical Degradation of Acid Blue 111 Using IrO_X Anode

S.Lj. Stupar[1], *B.N. Grgur*[1], *A.E. Onjia*[2], *D.Ž. Mijin*[1,*]

[1] Faculty of Technology and Metallurgy, University of Belgrade, Karnegijeva 4, 11020 Belgrade, Serbia
[2] Vinča Institute of Nuclear Sciences, University of Belgrade, P.O.Box 522, 11001 Belgrade, Serbia
[*]E-mail: BNGrgur@tmf.bg.ac.rs kavur@tmf.bg.ac.rs

Received: 20 June 2017 / *Accepted:* 10 July 2017 / *Published:* 13 August 2017

The anthraquinone dye, C.I. Acid Blue 111, was subjected to electrochemical oxidation using an IrOx electrode and sodium sulphate or sodium chloride as electrolytes. The effects of different operating parameters on the rate of dye decolorization, such as applied current, electrolyte concentration, and initial pH were studied. The dye concentration during the study was followed via ultraviolet-visible spectroscopy. The changes in the dye molecule during electrochemical oxidation were analyzed by Fourier Transformation-infrared spectroscopy. The level of mineralization after electrochemical oxidation was established by total organic carbon analysis.

Keywords: sodium chloride; sodium sulphate; UV/Vis spectroscopy; infrared spectroscopy; decolorization

1. INTRODUCTION

Wastewater from the textile industry after releasing in the environment, has hazardous effects on living organisms. The textile wastewater has high coloration, a high value of BOD/COD and TDS loads, hence all of these cause imbalance in the environment [1,2]. Dyes with the anthraquinone chromophore, the group which C.I. Acid Blue 111 ($C_{31}H_{25}N_2NaO_7S$, CAS 6420-90-4, C.I.62155, AB111, Figure 1) belongs to, have a toxic influence towards microorganisms. High toxicity for microorganisms inhibits biological treatment during the nitrification/denitrification steps, and conventional wastewater treatment plants with biological reactors are not able to entirely remove these kinds of pollutants [3].

Nowadays, many technologies which are environmentally-friendly are being developed for the treatment of textile industry wastewater: advanced oxidation processes [4], direct or indirect electrochemical oxidation of effluent [5-7], adsorption [8], biological treatment [9].

In the past years, research efforts have been made in developing more effective technologies to completely remove persistent and emerging man-made organic chemicals from wastewater. Among new developed processes, electrochemical oxidation is a promising one, and can be considered as clean, because this process involves electrons and oxidation agents produced *in situ* as reagents for the degradation of organic compounds from effluents. Other advantages of this process include the use of simple equipment, easy operation, robustness, versatility and viability for automation [6,7,10].

In the past decade, electrochemical oxidation showed high effectiveness in decolorizing and eliminating dye molecules from water solutions [10-13]. Electrochemical oxidation can be separated into two types, direct and indirect electrochemical oxidation [6,10].

During the process of direct electrochemical oxidation, organic compounds exchange electrons directly with the anode surface. This method is not very effective in the degradation of pollutants because of the deactivation of the electrode due to the formation of a polymeric layer on the surface of the anode. Direct electrochemical oxidation treatment of industrial effluents is based on the elimination of organic compounds directly in the vicinity of the surface of the anode and/or production of the hydroxyl radicals, $^{\bullet}OH$.

The hydroxyl radical mediation can promote the partial oxidation and selective oxidation of the organic pollutant and also its complete mineralization, depending on the anode material and salt-containing wastewaters [14,15]. Comninellis [16] has proposed a model for the oxidation of organic compounds with hydroxyl radicals, considering the existence of two types of anodes, the “active” and the “non-active” ones. Some of the “active” anodes that can be used are Pt, IrO_2 and RuO_2. On the other hand “non-active” anodes are made from materials such as PbO_2, SnO_2 and boron-doped diamond. The difference between these two types of electrodes is that a “non-active” electrode does not provide any catalytic active sites for the adsorption of reactants and/or products from the aqueous medium. In these processes, the anode serves only as an inert substrate, which can act as a collector to remove the electrons [17]. In the recent past, widely used materials for anodes in electrochemical degradation treatments are mixed metal oxides of Ir, Sn, Ti, Sb [18-20].

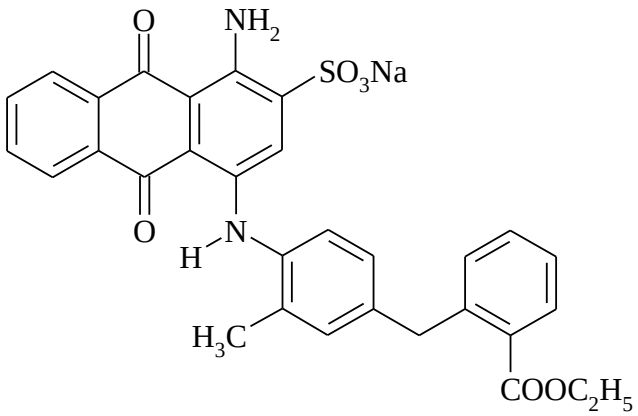

Figure 1. C.I. Acid Blue 111 structure.

From a kinetic point of view, the indirect oxidation is more effective in comparison to the direct one [12]. The basic indirect oxidation agent used in wastewater degradation treatment is active chlorine (a mixture of Cl_2, HClO, ClO^-) [2,14,21], which can be easily obtained by the electrolysis of chloride containing solutions.

The aim of this study was the investigation of the electrocatalytic degradation of C.I. Acid Blue 111 from a simulated wastewater using an IrO_2 anode in the presence of NaCl and Na_2SO_4. IrO_2 based anodes are dimensionally stable electrode (DSA/type electrodes) types with excellent electro-catalytic activity for O_2 and Cl_2 evolutions. The main characteristics of IrO_2 are the low price of the material, enhanced catalytic activity for degradation processes, and stability against corrosion compared to some other electrodes like RuO_2 [22]. IrO_2 electrodes have been used in electrochemical degradation of various dyes: Acid Orange 7 [23], Crystal Violet [24], Indigo Carmine [25], Acid Orange 2 [26], Reactive Red 120 [27], Brilliant Red X-3B [28], or dye effluents [29].

According to our knowledge, AB111 has not been subjected to any electrochemical treatment. So, we have studied the effect of different operating parameters on the rate of dye decolorization such as applied current, electrolyte concentration, and initial pH. The dye concentration during the study was followed via ultraviolet-visible (UV/Vis) spectroscopy. A Fourier Transformation-infrared (FTIR) study was used to establish the changes in the AB111 molecule. Total organic carbon (TOC) analysis provided the information on the level of dye mineralization after electrochemical oxidation.

2. EXPERIMENTAL PART

2.1. Materials and methods

The AB111 dye was obtained from Hoechst A.G. (Germany), trade name Alphanol Fast Blue FGLL. NaCl was purchased from Zdravlje, Leskovac, Serbia and Na_2SO_4 from Centrohem, Serbia. H_2SO_4 and NaOH were obtained from Sigma-Aldrich (USA). All chemicals were at least of analytical grade and were used without any further purification treatments. Deionized water was obtained using the Milipore Waters Milli-Q (USA) purification system. As the current source, a PAR M273 potentiostat/galvanostat in the galvanostatic mode was used, and was received from Iskra (Slovenia). The ampere meter was also produced by Iskra (Slovenia). The IrO_x-anode was produced by De Nora (5 cm^2) (USA). The dye concentration was followed using a UV/Vis Shimadzu 1800 spectrophotometer (Japan). The pH measurements were performed using a Hanna pH Meter HI-2210 (Italy). The magnetic stirrer was produced by Heidolph (Germany). The IR spectra were obtained using a Bomem MB-Series 100 (USA) Fourier Transformation-infrared spectrophotometer in the form of KBr pellets. Samples were prepared by the extraction of an electrolyte solution, after 60 minutes (sodium sulphate) and 30 minutes (sodium chloride) of reaction, with diethyl ether (Sigma-Aldrich, USA). Ether solutions were dried using anhydrous sodium sulphate (Kemika, Croatia) and afterwards evaporated. The total organic carbon (TOC) analysis during the electrolysis was determined using ZellwegerLabTOC 2100 (USA).

2.2. Electrochemical degradation

The electrochemical oxidations were performed in an open reactor at room temperature (~25 ºC) with an electrolyte volume of 200 cm^3. The concentration of the AB111 dye in the water solution was 100 mg dm^{-3}. A typical experiment included the preparation of the electrolyte using deionized water, salt (NaCl or Na_2SO_4) and AB111. As the cathode, a 10 cm^2 plate made from austenite 18Cr/8Ni stainless steel series 304 was used. Both electrodes (IrO_x and stainless steel) were immersed in the electrolyte (at the top of the reactor, with the electrode gap of 3 mm). The electrolyte was mixed by the magnetic stirrer. The reaction was followed by UV/Vis spectrophotometry.

Dye degradation was investigated at pH of dye solution, as well as at pH 3 and pH 12. The value of pH was adjusted by the addition of 0.1 mol dm^{-3} H_2SO_4 for pH 3 or the same concentration of NaOH solution for pH 12.

3. RESULTS AND DISCUSSION

3.1. Direct electrochemical oxidation of AB111

Direct electroxidation of AB111 was studied in the presence of sodium sulphate as the electrolyte. For the IrO_x anode in direct oxidation of the organic molecule, the first reaction (Eq. 1) is the oxidation of water molecules on the electrode surface leading to the formation of adsorbed hydroxyl radicals [14,30]:

$$M + H_2O \rightarrow M\text{-}(^{\bullet}OH)_{ads} + H^+ + e^- \quad (1)$$

The active electrodes are characterized by a strong interaction between the electrode (M) and the hydroxyl radical ($^{\bullet}OH$), so the adsorbed hydroxyl radicals may form so called higher oxides (MO) on the anode (Eq. 2).

$$M(^{\bullet}OH)_{ads} \rightarrow MO + H^+ + e^- \quad (2)$$

The redox couple MO/M participates in the selective oxidation of organic compounds (R) without complete incineration (Eq. 3).

$$MO + R \rightarrow M + RO \quad (3)$$

As a result of the chemical decomposition of the higher oxide, the side reaction of oxygen evolution (Eq. 4) competes with the reaction given by Eq. 3.

$$2MO \rightarrow 2M + O_2 \quad (4)$$

The effect of the applied current, electrolyte concentration and initial pH of the electrolyte solution on the direct electrochemical oxidation of AB111 was studied. Figure 2 shows the results of the applied current influence on the electrochemical oxidation of AB111. The studied reaction can be well described using the pseudo first-order rate constant, k, min^{-1}:

$$\ln\frac{C}{C_0} = -k \cdot t \quad (5)$$

where C represents the dye concentration at a specific time, while C_0 is the dye concentration at zero time. C/C_0 represents normalized concentration.

The current varied between 100 and 300 mA and the obtained results indicated that an increase in the applied current increases the reaction rate. This is in agreement with the results obtained by de Oliveira Morais et al. [31] which reported that an increase in applied current density using a $Ti/Ru_{0.34}Ti_{0.66}O_2$ anode (active anode), which led to an increase in color removal. The increase in applied current increases the formation of adsorbed radicals (Eq. 1) as well as higher oxides (Eq. 2). The parallel reaction is oxygen evolution (Eq. 4). Also, the adsorption of the dye is important to achieve the electrooxidation of the organic molecule. The increased oxidation rate is due to the increased direct electron transfer between the electrode surface and the adsorbed dye molecules [32,33].

In addition, one can calculate the energy consumption per volume of dye solution using Eq. 6 in kWh m^{-3} [34]:

$$Energy\ consumption = \frac{U \cdot I \cdot t}{V_S} \quad (6)$$

where t is a time of electrolysis in hours, U, V is cell voltage, I is current, and V_s is the sample volume in m^3. Here, during the change in the initial reaction rate from 0.0045min^{-1} to 0.0162 min^{-1}, the energy consumption increases from 0.75 to 2.5 kWh m^{-3} (cell voltage change from 3 to 4.25 V). Although the reaction is fastest at the highest applied current (3.6 times), it is more economical to use lower currents.

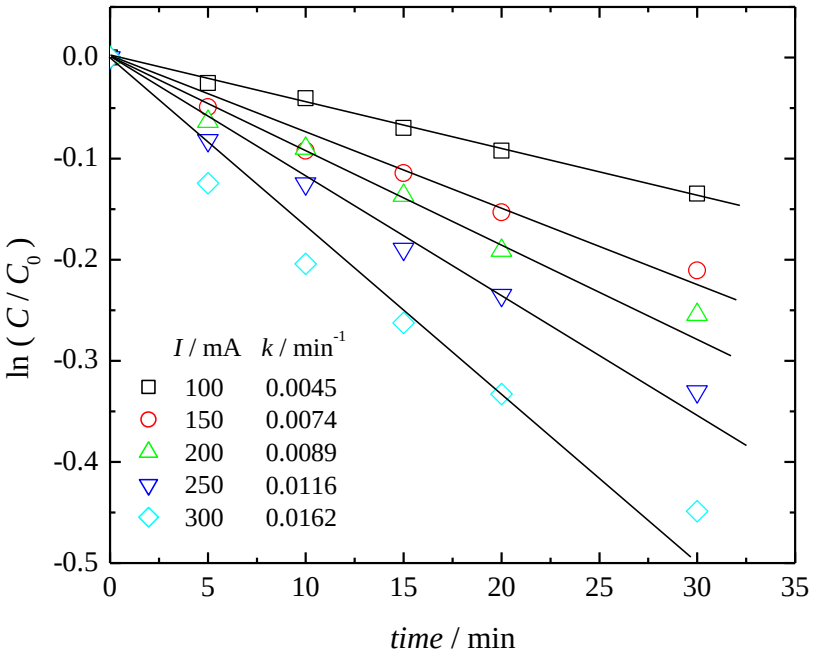

Figure 2. The logarithmic plot of the relative concentration of AB111 versus the electrolysis time for different values of the applied current (marked in the figure). Conditions C_{Na2SO4} = 0.17 M, C_{AB111} = 100 mg dm^{-3}, ω = 800 rpm.

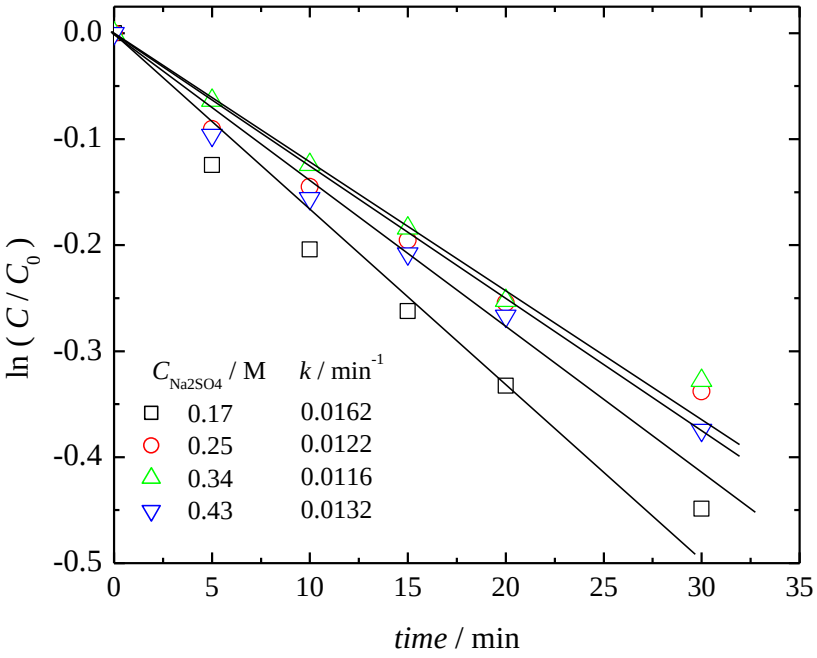

Figure 3. The logarithmic plot of the relative concentration of AB111 versus the electrolysis time for different values of sodium sulphate concentrations (marked in the figure). Conditions C_{AB111} = 100 mg dm^{-3}, I = 300 mA, ω = 800 rpm.

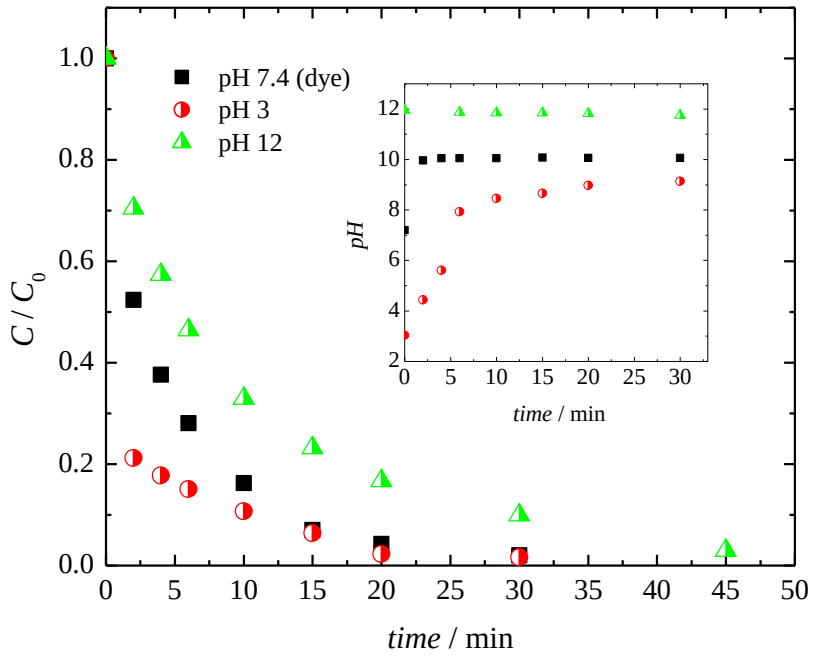

Figure 4. The relative concentrations of AB111 versus the electrolysis time for different values of pH (marked in the figure). Insert: The pH change during reactions with different initial pH values under conditions C_{Na2SO4} = 0.17 M, C_{AB111} = 100 mg dm^{-3}, I = 300 mA, ω = 800 rpm.

The influence of the initial electrolyte concentration was studied in the range of 0.17 – 0.43 M of sodium sulphate. As can be seen from Figure 3, the highest reaction rate was achieved with the lowest concentration used. This is the result of increased oxygen evolution (Eq. 4), due to the increased formation of adsorbed radicals (Eq. 1). The obtained results confirm that the oxygen evolution reaction proceeds rather than the oxidation of organic molecules when the IrOx electrode is used [32].

The influence of the initial pH of the electrolyte solution was studied by the addition of H_2SO_4 at pH 3 or by the addition of NaOH at pH 12 as well as at pH=7.4 of the dye solution. The obtained results are presented in Figure 4. An initial increase in pH of the electrolyte was observed due to the formation of OH^- ions during electrolysis at neutral and basic conditions (insert in Figure 4). The decrease of pH can be attributed to the degradation of dye molecules and the formation of acidic species [35]. The difference in reactivity of the AB111 dye at various initial pH of the solution might be the result of possible amino-imino tautomerism in the dye molecule [36].

3.2. Indirect electrochemical oxidation of AB111

The indirect electrochemical oxidation of the AB111 dye was performed using sodium chloride. "Active" chlorine is formed from a solution according to the following mechanism [37,38]:

- the first step is the oxidation of the chloride anions to hydrated chlorine, given by the overall reaction:

$$2Cl^- = Cl_2(aq) + 2e \quad (7)$$

- the second step is the fast hydrated chlorine disproportionation to HOCl followed by dissociation to OCl^-:

$$Cl_2(aq) + H_2O = HClO + Cl^- + H^+ \qquad K_1 = 5.1\times10^{-4}\ M^{-2} \quad (8)$$

$$HClO = ClO^- + H^+ \qquad K_a = 2.9\times10^{-8}\ M \quad (9)$$

The influence of the applied current on indirect electrooxidation was performed first. The applied current varied in the range 100-300 mA and the obtained results are given in Figure 5. As can be seen, there is an increase of the pseudo first-order rate constant (Eq. 5) with the increase of the applied current. And here the energy consumption can be calculated. During the change in the initial reaction rate from 0.0835 min^{-1} to 0.1887 min^{-1}, the energy consumption increases from 0.875 to 2.97 kWh m^{-3} (cell voltage change from 3.5 to 5.25 V). As with direct electrooxidation, the reaction is fastest at the highest applied current (2.25 times) but it is more economical to use lower currents.

The effect of salt concentration on the degradation process was tested at five different concentrations (0.17 - 0.51 M) at a constant current of 300 mA, and the results are shown in Figure 6. The reaction rate should be independent of chloride concentration because the amount of the produced active chlorine should be proportional to the passed charge (Faraday law). However, there is a competition between the oxygen evolution:

$$4OH^- = O_2 + 2H_2O + 4e^- \quad (10)$$

and the production of active chlorine [38,39].

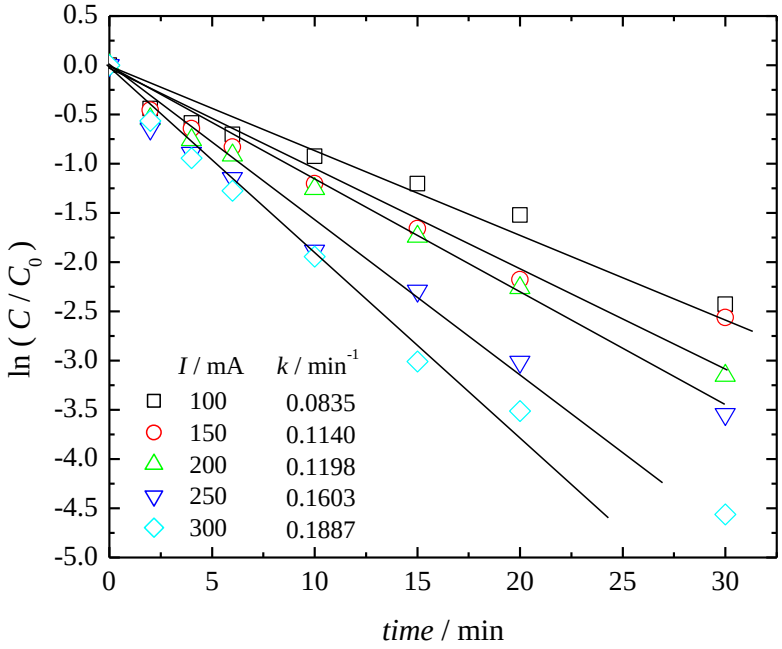

Figure 5. The logarithmic plot of the relative concentrations of AB111 versus the electrolysis time for different values of the applied current (marked in the figure). Conditions C_{NaCl} = 0.17 M, C_{AB111} = 100 mg dm^{-3}, ω = 500 rpm.

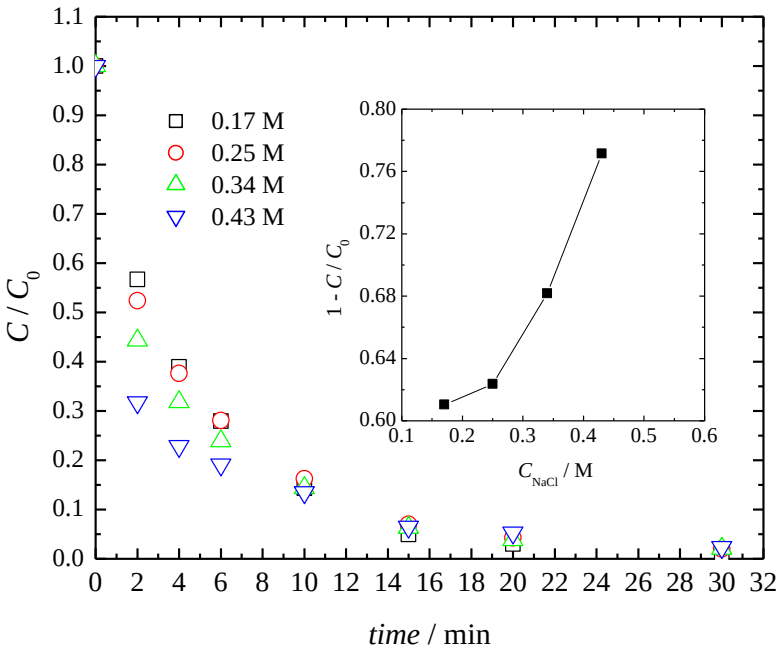

Figure 6. The relative concentrations of AB111 versus the electrolysis time for different values of sodium chloride concentrations (marked in the figure). Insert: The influence of sodium chloride concentrations on the efficiency of the electrolysis of AB111 under conditions C_{AB111} = 100 mg dm^{-3}, I = 300 mA, ω = 500 rpm.

Besides, the reaction rate could not be well described by the pseudo first-rate order so instead, the discoloration efficiency was calculated by Eq. 11:

$$Efficiency = 1\text{-}C/C_0 \quad (11)$$

For example, after 2 minutes of the reaction, one can calculate that the highest efficiency was with 0.43 M of sodium chloride. This is also true for the initial part of the reaction (up to 10 min). But, from a practical point, a lower concentration may be used: the efficiency rose by ~18% while the sodium chloride concentration increased 2.5 times.

The electrochemical oxidation of AB111 in the presence of sodium chloride was additionally studied at a different pH (Figure 7). It is known that there is a mixture of chlorine, hypochlorous acid and hypochlorite in the system depending on the pH value [40]. Namely, at lower pH values (below 5), chlorine molecules and hypochlorous acids exist, while at higher pH values (above 10) the only species is hypochlorite. So, at pH 3 hypohlorous acid is an active species in AB111 decolorization and the reaction proceeds fastest. As pH is increased, the dissociation of hypochlorous acid to hypochlorite occurs. This leads to a decrease in the reaction rate and the reaction is slower when the AB111 solution (without added acid) is electrolyzed. A further increase in the initial pH value will increase the hypochlorite concentration and the reaction will be slower. A similar behavior was observed in the electrochemical decolorization of CI Basic Yellow 28 [41] and CI Reactive Orange 16 [40].

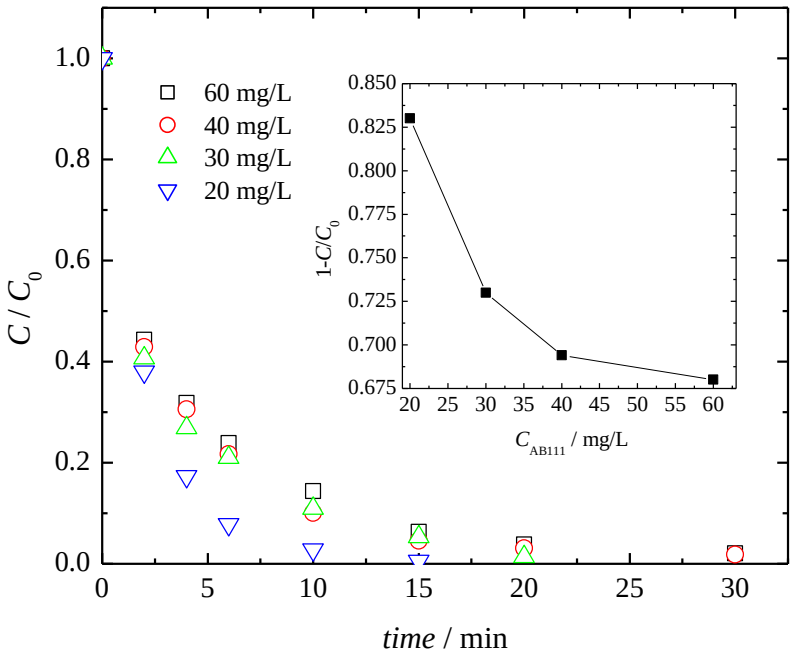

Figure 7. The relative concentrations of AB111 versus the electrolysis time for different values of pH (marked in the figure). Insert: The pH change during reactions with different initial pH values under conditions C_{NaCl} = 0.17 M, C_{AB111} = 100 mg dm^{-3}, I = 300 mA, ω = 500 rpm.

It can be concluded that when IrOx is used in the electrooxidation of AB111 in the presence of sodium sulphate and sodium chloride, the reaction proceeds much faster in the presence of sodium chloride, and that decolorization can be achieved after 30 min of electrolysis.

3.3. UV/Vis, FTIR and TOC study

3.3.1. UV/Vis spectra change

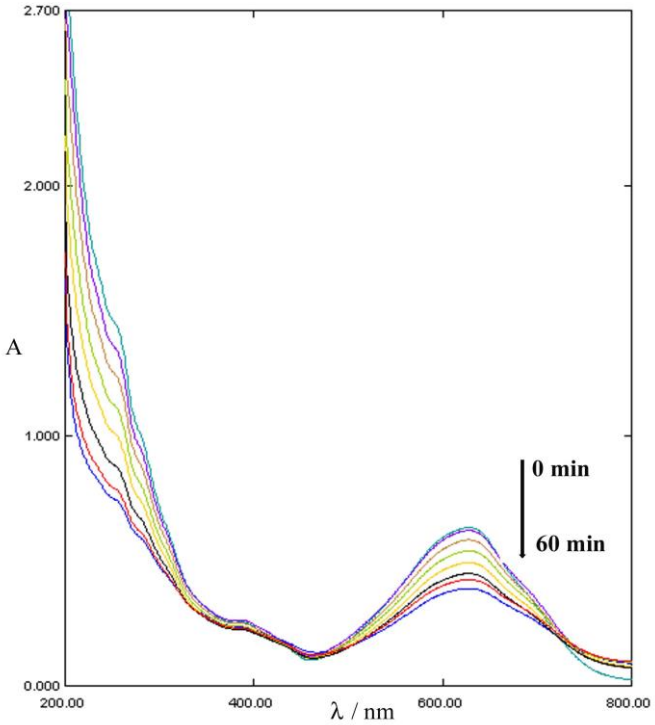

Figure 8. Typical UV/Vis spectra changes of B111 during direct electrochemical treatment: conditions C_{Na2SO4} = 0.17 M, C_{AB111} = 100 mg dm^{-3}, I = 300 mA, pH 3, ω = 800 rpm.

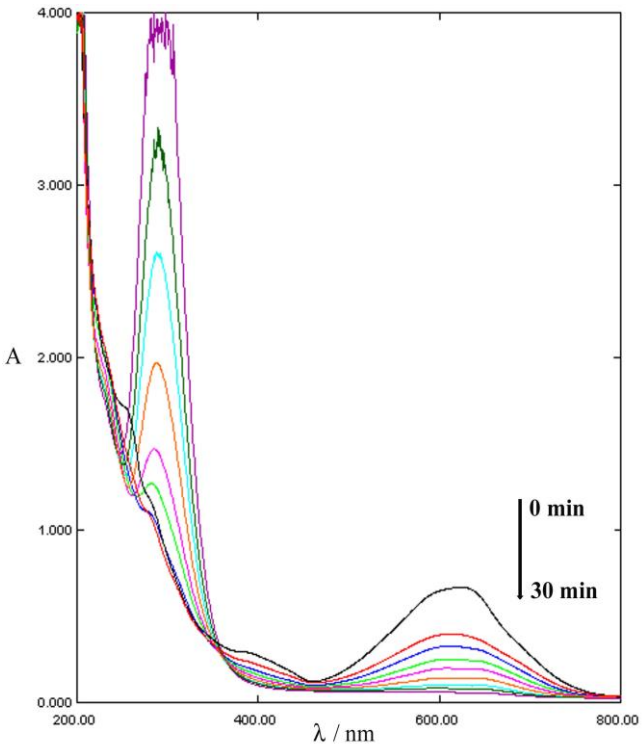

Figure 9. Typical UV/Vis spectra changes of B111 during indirect electrochemical treatment: conditions C_{NaCl} = 0.43 M, C_{AB111} = 100 mg dm^{-3}, I = 300 mA, ω = 500 rpm.

The reaction of decolorization of AB111 was followed by using UV-Vis spectroscopy and Figures 8 and 9 give the UV/Vis spectra changes during electrolysis. AB111 has the absorption maximum at a wavelength of 634 nm. The decrease of the absorption peak during electrolysis indicates the decolorization of AB111 dye over time. When sodium chloride was used, a complete decolorization was observed after 30 min of electrochemical treatment (Figure 9). In contrast, the reaction with sodium sulphate proceeds slower and after 60 minutes of electrochemical treatment, there were still dye molecules present in the system (Figure 8). A generation of hypochlorite, during indirect electrolysis, can be observed (Figure 9) since hypochlorite has the absorption maximum at 292 nm [42].

3.3.2. FTIR study

The electrochemical degradation of the AB111 dye was also studied using FTIR spectroscopy. Samples were prepared by the extraction of the electrolyte solution with diethyl ether as described in the Experimental part.

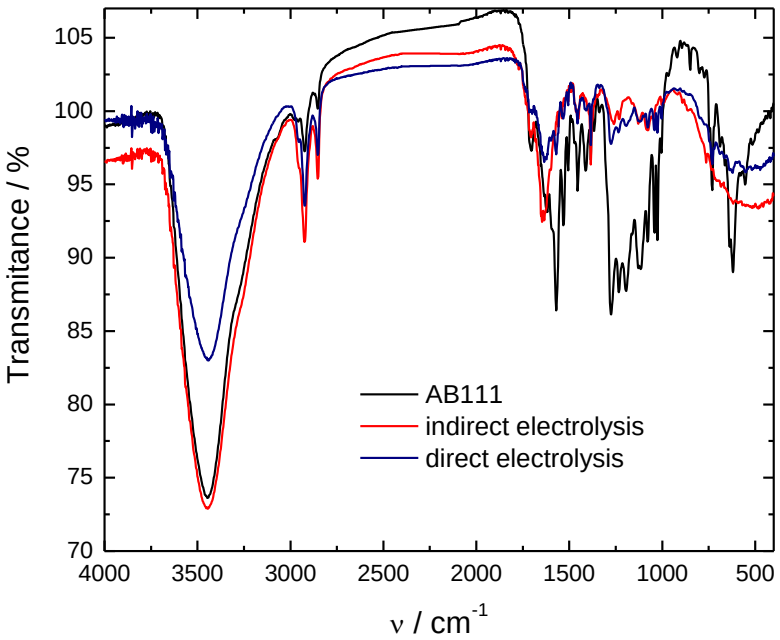

Figure 10. The FTIR spectra of AB111 and extracts obtained after the electrochemical degradation of AB111 (C_{NaCl} = 0.17 M, C_{Na2SO4} = 0.17 M, C_{AB111} = 100 mg dm^{-3}, I = 300 mA, ω = 500/800 rpm).

The absorptions in FTIR spectra of AB111 (Figure 10) at 3448 cm^{-1} can be attributed to –OH or –NH_2, while the shoulder at ~3330 cm^{-1} originates from –NH_2. Two absorption peaks at 2922 and 2855 cm^{-1} as well as at 729 cm^{-1} can be assigned to C-H aliphatic vibrations. The peak at 1699 cm^{-1} belongs to the ester C=O, while absorption at 1630 cm^{-1} can be attributed to the C=O group. The

absorption at 1569, 1506 and 1450 cm^{-1} can be assigned to C=C of the quinonoid system. The peak at 1410 cm^{-1} originate from aromatic C-H vibration. The absorption peak at 1330 cm^{-1} can be attributed to C-N vibrations. Peaks between 1273 and 1115 cm^{-1} can be assigned to C-O and $–SO_3H$. The absorption at 1076 cm^{-1} can be also assigned to $–SO_3H$ [43]. The difference in the IR absorptions obtained for the AB111 dye and the products of electrooxidation is the increase in absorption intensities of aliphatic vibrations at 2922 and 2855 cm^{-1} for direct and indirect oxidation. Also, there is an increase in absorption at 1382 cm^{-1} (CH_3) and the disappearance of the absorption peak at 729 cm^{-1} (C-H) after indirect oxidation. In addition, there is a change in carbonyl frequency from 1630 to 1645 cm^{-1} in indirect oxidation, indicating a change in the quinone group. The disappearance of the absorption peak at 1569 cm^{-1} indicates a change in aromatic structure during indirect oxidation. A decrease in absorption intensity was observed for both products in the region between 1273 and 1115 cm^{-1} indicating the probable cleavage of C-O bonds.

3.3.3. TOC analysis

In addition, the electrochemical degradation of the AB111 dye was studied using TOC analysis in order to establish the effectiveness of the used method. TOC analysis was performed for samples obtained after direct (60 min) and indirect (30 min) electrochemical treatment (Figure 11). As can be seen from Figure 11, a higher degree of mineralization was achieved during indirect degradation, as expected. Although the UV-Vis data (Figure 6) indicates an almost complete removal of the dye during indirect electrolysis, TOC results showed that only 65% of the dye was mineralized after 30 min. On the other hand, after 1 h of direct electrolysis TOC results showed that only 24% of the dye was mineralized while UV-Vis data (Figure 4) indicated that degradation was around ~45%.

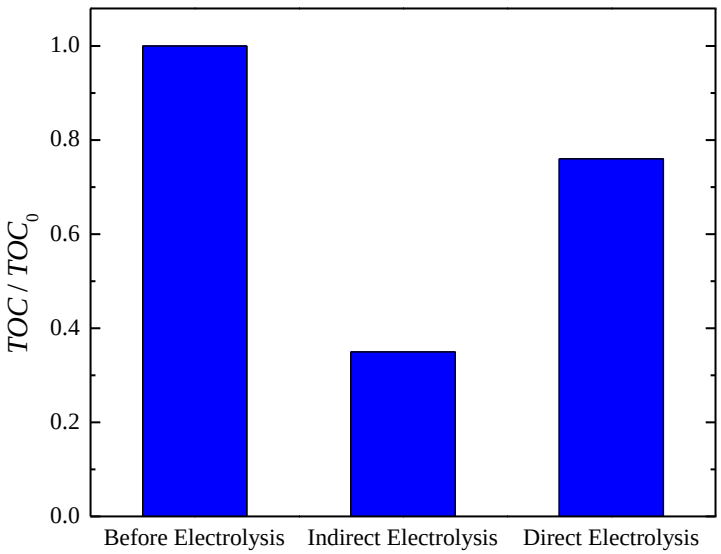

Figure 11. TOC analysis of AB111 solution and solutions after the electrochemical degradation of AB111 (C_{NaCl} = 0.17 M, C_{Na2SO4} = 0.17 M, C_{AB111} = 100 mg dm^{-3}, I = 300 mA, ω = 500/800 rpm)

4. CONCLUSION

During direct oxidation of the AB111 dye, it was found out that the pseudo first reaction rate constant increases with the increase of the applied current. Although the reaction proceeds faster with the higher applied current, it is more economical to use lower currents. When the initial sodium sulphate concentration was varied it was discerned that the optimal concentration should be the lowest one (0.17 M). The initial pH value of the electrolyte had small influence on the reaction rate. The difference in the reactivity of the AB111 dye at various initial pH values of the solution might be the result of possible amino-imino tautomerism in the dye molecule.

During indirect oxidation of AB111, it was also discerned that there is an increase of the pseudo first-order rate constant with the increase of the applied current. As with direct electrooxidation, the reaction is fastest at the highest applied current, but it is more economical to use lower currents. Although the highest reaction efficiency was with 0.43 M of sodium chloride, from a practical point of view, a lower concentration may be used. The highest reaction rate was obtained at pH 3 while the reaction rate was lowest at pH 12, due to the different active species involved.

The obtained results showed that when IrOx is used in the electrooxidation of AB111 in the presence of sodium sulphate and sodium chloride, the reaction proceeds much faster in the presence of sodium chloride, and the complete decolorization can be achieved after 30 min of electrolysis.

The IR data of the AB111 dye and the products of electrooxidation revealed an increase in the number of aliphatic C-H bonds, a change in aromatic structure, the probable cleavage of C-O bonds and a change in the quinone group.

Although UV-Vis data indicates an almost complete removal of dye during indirect electrolysis, TOC results showed that only 65% of the dye was mineralized after 30 min. On the other hand, after 1 h of direct electrolysis TOC results showed that only 24% of the dye was mineralized while UV-Vis data indicated that degradation was around ~45%.

ACKNOWLEDGEMENT:
The work was supported by the Ministry of Education and Science of the Republic of Serbia under the research projects: ON172013 and ON172046.

References

1. C. R. Holkar, A. J. Jadhav, D. V. Pinjari, N.M. Mahamuni, A. B. Pandit, *J. Environ. Manage.*, 182 (2016) 351.
2. C.A Martinez-Huitle, E. Brillas, *Appl. Catal., B*, 87 (2009) 105.
3. M.E. Argun, D. Guclu, M. Karatas, *J. Ind. Eng. Chem*., 20 (2014) 1079.
4. L. Bilinska, M. Gmurek, S. Ledakowicz, *Chem. Eng. J*., 306 (2016) 550.
5. N.E.H. Abdessamad, H. Akrout, G. Hamdaoui, K. Elghniji, M. Ksibi, L. Bousselmi, *Chemosphere*, 93 (2013) 1309.
6. J.H.B. Rocha, M.M.S. Gomes, E.V. dos Santos, E.C.M. de Moura, D.R. da Silva, M.A. Quiroz, C.A. Martínez-Huitle, *Electrochim. Acta*, 140 (2014) 419.
7. Y. Zhang, T. Yu, W. Han, X. Sun, J. Li, J. Shen, L. Wang, *Electrochim. Acta*, 220 (2016) 211.

8. A. Hassani, A. Khataee, S. Karaca, M. Karaca, M. Kıranşan, *J. Environ. Chem. Eng*., 3 (2015) 2738.
9. E. Sahinkaya, A. Yurtsever, O. Cınar, *Sep. Purif. Technol*., 174 (2017) 445.
10. C. Zhang, J. Tang, C. Peng, M. Jin, *J. Mol. Liq*., (2016) 1145.
11. F.C. Moreira, R.A.R. Boaventura, E. Brillas, V.J.P. Vilar, *Appl. Catal., B*, 202 (2017) 217.
12. C. Zhang, L. Lui, W. Li, J.Wu, F. Rong, D. Fu, *J. Electroanal. Chem*., 726 (2014) 77.
13. F. Zhang, C. Feng, W. Li, J. Cui, *Int. J. Electrochem. Sci*., 9 (2014) 943.
14. C.A. Martínez-Huitle, S. Ferro, *Chem. Soc. Rev*., 35 (2006) 1324.
15. A. Fernandes, M.J. Pacheco, L. Ciriaco, A. Lopes, *Appl. Catal., B*, 176-177 (2015) 183.
16. C. Comninellis, *Electrochim. Acta*, 39 (1994) 1857.
17. A. Benito, A. Penades, J.L. Lliberia, R. Gonzalez-Olmos, *Chemosphere*, 166 (2017) 230.
18. S. Song, J. Fan, Z.He, L. Zhan, Z. Liu, J. Chen, X. Xu, *Electrochim. Acta*, 55 (2010) 3606.
19. H. An, H. Cui, W. Zhang, J. Zhaim Y. Qian, X. Xie, Q. Li, *Chem. Eng. J*., 209 (2012) 86.
20. A. Papaderakis, D. Tsiplakides, S. Balomenou, S. Sotiropoulos, *J. Electroanal. Chem*., 757 (2015) 216.
21. I. Sirés, E. Brillas, M.A. Oturan, M.A. Rodrigo, M. Panizza, *Environ. Sci. Pollut. Res. Int*., 21 (2014) 8336.
22. F. Zaviska, P. Drogui, J.F. Blais G. J. Mercier, *J. Appl. Electrochem*., 39 (2009) 2397.
23. J. Feng, S. Lan, C. Yao, Y. Xiong, S. Tian, *J. Chem. Technol. Biotechnol*., 92 (2017) 827.
24. F.L. Guzmán-Duque, R.E. Palma-Goyes, I. González, G. Peñuela, R.A. Torres-Palma, *J. Hazard. Mater*., 278 (2014) 221.
25. R.E. Palma-Goyes, J. Silva-Agredo, I. Gonzalez, R.A. Torres -Palma, *Electrochim. Acta*, 140 (2014) 427.
26. F. Zhang, W. Li, C. Feng, L. Yu, C. Zhao, G. Hao, *Shuichuli Jishu*, 37 (2011) 77.
27. T. Panakoulias, P. Kalatzis, D. Kalderis, A. Katsaounis, *J. Appl. Electrochem*., 40 (2010) 1759.
28. X.-N. Wang, J.-P. Jia, Y.-L. Wang, *Ultrason. Sonochem*., 17 (2010) 515.
29. K. Rathinakumaran, R.M. Meyyappan, *Int. J. Chem. Sci*., 13 (2015) 1401.
30. H.S. Awad, N.A. Galwa, *Chemosphere*, 61 (2005) 1327.
31. C.C. de Oliveira Morais, A.J.C. da Silva, M.B. Ferreira, D.M. de Araújo, *Electrocatalysis*, 4 (2013) 312.
32. J.L. Nava, M.A. Quiroz, C.A. Martínez-Huitle, *J. Mex. Chem. Soc*., 52 (2008) 249.
33. A.J.C. da Silva, E.V. dos Santos, C.C. de Oliveira Morais, C.A. Martínez-Huitle, S.S.L. Castro, *Chem. Eng. J*., 233 (2013) 47.
34. J.H.B. Rocha, N.S. Fernandes, K.R. Souza, D.R. da Silva, M.A. Quiroz, C.A. Martínez-Huitle, *Sustain. Environ. Res*., 21 (2011) 291.
35. E. Brillas, C.A. Martínez-Huitle, *Appl. Catal., B*, 166–167 (2015) 603.
36. V.Ya. Fain, B.E. Zaitsev, M.A. Ryabov, *Russ. J. Org. Chem*., 45 (2009) 374.
37. A. Kraft, M. Stadelmann, M. Blaschke, D. Kreysig, B. Sandt, F. Schroéder, J. Rennau, *J. Appl. Electrochem*., 29 (1999) 861.
38. M.A. Rauf, S.S. Ashraf, *Chem. Eng. J*., 151(2009) 10.
39. J.P. Lorimer, T.J. Mason, M. Plattes, S.S. Phull, D. Walton, *Pure Appl. Chem*., 73 (2011) 1957.
40. D.Ž. Mijin, V.D. Tomić, B.N. Grgur, *J. Serb. Chem. Soc*., 80 (2015) 903.
41. D.Ž. Mijin, M.L. Avramov Ivić, A.E. Onjia, B.N. Grgur, *Chem. Eng. J*., 204–206 (2012) 151.
42. L.C. Adam, I. Fábián, K. Suzuki, G. Gordon, *Inorg. Chem*., 31 (1992) 3534.
43. M.M.A. Sekkina, S.S. Assar, *Pros. Indian natn. Sci. Acad*., 48 (1982) 112.